PHYSICAL REVIEW D VOLUME 44, NUMBER 10 15 NOVEMBER 1991

Static heavy-quark potential calculated in the classical approximation to dual QCD

M. Baker
University of Washington, Seattle, Washington 98105

James S. Ball
University of Utah, Salt Lake City, Utah 84112

F. Zachariasen
California Institute of Technology, Pasadena, California 91125
(Received 20 May 1991)

We use the classical approximation to dual QCD to compute the distribution of color fields around heavy quarks and the static potential between them. The resulting potential is in excellent agreement with phenomenologically obtained ones. As the distance between the quark-antiquark pair increases, the color field lines evolve from a squashed dipole distribution to a flux-tube distribution. It is noteworthy that the potential becomes linear well before the appearance of a fully developed flux tube. A comparison of these field distributions with lattice Monte Carlo calculations could test quantitatively whether dual superconductivity is the physical mechanism for confinement in QCD.

I. INTRODUCTION

Dual QCD is ordinary QCD expressed in terms of dual (electric) vector potentials C_μ^a rather than the conventional (magnetic) vector potentials A_μ^a [1]. At present, it is not possible to write down the exact QCD Lagrangian as a function of the dual fields C_μ^a (indeed, it is conceivable that it is, in principle, impossible [2]). Nevertheless, a phenomenological dual QCD Lagrangian does exist and respects all of the necessary properties of a respectable field theory at low energies and at the classical or tree approximation level [2]. Practical calculations can therefore be undertaken in dual QCD, and our purpose in this paper is to report one such calculation, namely, the evaluation of the static quark-antiquark potential in the classical approximation. This is very similar to the calculation of the force between a magnetic monopole and an antimonopole in the Landau-Ginzburg approximation to superconductivity [3], which should come as no surprise since the phenomenological QCD Lagrangian describes a dual superconductor, and color confinement is the analogue of the Meissner effort.

Earlier calculations of the static quark-antiquark potential in QCD have been carried out using the bag model (both the conventional MIT bag [4] and the dual QCD analogue of it [5]) and using lattice methods [6]. These calculations all produce potentials in good agreement with those found phenomenologically [7], and, as we will see, the calculation presented here does too. Nevertheless, it is of value to compute things using as many different techniques as possible because some techniques may be more easily extended to new calculations than others. The calculation we shall describe here, since it is classical, precludes our introducing quarks carrying the usual color matrices $\lambda^a/2$. Instead, we shall use Abelian sources with charge e. (Note that, at the classical level, attaching color matrices to fixed sources makes no sense, since the relative color orientation of the sources can be changed by a gauge transformation. Further, since we do not, in dual QCD, know how to deal with quarks beyond lowest order [8] in the dual coupling constant g, we shall ignore higher-order (in g) couplings of quarks to the dual QCD fields.)

II. THE DUAL QCD CLASSICAL FIELD EQUATIONS WITH QUARK SOURCES

Because dual QCD is set up in terms of dual potentials, the introduction of color-electric sources requires some delicacy. How quark sources are introduced has been described elsewhere [8], nevertheless, for the sake of writing a self-contained paper, we repeat part of the discussion here.

The usual definition of the electric displacement $\mathbf{D}$ in terms of the dual potential $\mathbf{C}$ implies the absence of color-electric sources (i.e., $\nabla\cdot\mathbf{D}=0$ because $\mathbf{D}=\nabla\times\mathbf{C}$). Therefore, in order to put in quark sources, the relationship between $\mathbf{D}$ and $\mathbf{C}$ must be modified. We write

$$\mathbf{D}=\nabla\times\mathbf{C}+\mathbf{D}_S\ , \tag{2.1}$$

and choose the "string field" $\mathbf{D}_S$ to satisfy

$$\nabla\cdot\mathbf{D}_S=\sum_i e_i\delta^3(\mathbf{x}-\mathbf{x}_i) \tag{2.2}$$

for a set of quarks of charge e_i located at positions $\mathbf{x}_i$. For a single quark, $\mathbf{C}$ is the usual Dirac monopole field: in spherical coordinates

$$\mathbf{C}\equiv\mathbf{C}_D=-e\frac{1+\cos\theta}{4\pi r\sin\theta}\hat{\mathbf{e}}_\varphi\ . \tag{2.3}$$

Here $e=2\pi/g$, where g is the dual coupling constant. Then, choosing the string along the z axis,

$$\mathbf{D}_S = e\delta(x)\delta(y)\theta(z)\hat{\mathbf{e}}_z \ , \tag{2.4}$$

which satisfies (2.2). Thus, Eq. (2.1) simply reflects the identity

$$\frac{e\hat{\mathbf{e}}_r}{4\pi r^2} = \nabla\times\left[-e\frac{1+\cos\theta}{4\pi r\sin\theta}\hat{\mathbf{e}}_\varphi\right] + e\delta(x)\delta(y)\theta(z)\hat{\mathbf{e}}_z \ . \tag{2.5}$$

The string field serves only to cancel the string present in $\nabla\times\mathbf{C}_D$: both $\nabla\times\mathbf{C}_D$ and $\mathbf{D}_S$ contain strings, but $\mathbf{D}$ does not, as is required physically.

Extending the above argument to a quark-antiquark pair, located on the z axis a distance R apart, we write [now in cylindrical coordinates (ρ,ϕ,z)]

$$\mathbf{C}_D = -\frac{e}{4\pi\rho}\left[\frac{z-R/2}{\sqrt{\rho^2+(z-R/2)^2}} - \frac{z+R/2}{\sqrt{\rho^2+(z+R/2)^2}}\right]\hat{e}_\phi \tag{2.6}$$

and

$$\mathbf{D}_S = e\delta(x)\delta(y)[\theta(z-R/2)-\theta(z+R/2)]\hat{e}_z \ , \tag{2.7}$$

where the string now joins the two charges (this represents a gauge choice). We note for future reference that

$$\tfrac{1}{2}\int d^3\mathbf{x}(\nabla\times\mathbf{C}_D+\mathbf{D}_S)^2 = -\frac{e^2}{4\pi R} + \text{self-energy terms} \ . \tag{2.8}$$

The dual QCD Lagrangain is

$$\mathcal{L}(C) = \tfrac{1}{4}\tilde{F}_{\mu\nu}\mathcal{D}^2\tilde{F}_{\mu\nu} - \tfrac{1}{4}G_{\mu\nu}G_{\mu\nu} - W(\tilde{F}) \ , \tag{2.9}$$

plus ghost and gauge-fixing terms [9]. Here

$$D_i^a = \tfrac{1}{2}\epsilon_{ijk}G_{jk}^a + D_{Si}^a \tag{2.10a}$$

is the electric displacement, and we define

$$H_i^a = G_{0i}^a \tag{2.10b}$$

as the magnetic field. The relationship of $G_{\mu\nu}$ to the dual potential C_μ is, as usual,

$$G_{\mu\nu}^a = \partial_\mu C_\nu^a - \partial_\nu C_\mu^a + g f^{abc}C_\mu^b C_\nu^c \ . \tag{2.11}$$

The auxiliary tensor $\tilde{F}_{\mu\nu}$ we write as

$$E_i^a = -\tfrac{1}{2}\epsilon_{ijk}\tilde{F}_{jk}^a \tag{2.12a}$$

and

$$B_i^a = -\tilde{F}_{0i}^a \ , \tag{2.12b}$$

in a notation which is meant to be suggestive. The function $W(\tilde{F})$ contains the counterterms necessary to make $\mathcal{L}(C)$ renormalizable; its explicit form is

$$W(\tilde{F}) = -\frac{\mu^2 N}{4}\tilde{F}^2 + \frac{N\lambda}{4!}W_4(\tilde{F}) \ , \tag{2.13}$$

where

$$\tilde{F}^2 = \tilde{F}_{\mu\nu}^a\tilde{F}^{\mu\nu a} = -2[(\mathbf{B}^a)^2-(\mathbf{E}^a)^2] \ , \tag{2.14}$$

and where $W_4(\tilde{F})$ is a quartic function of $\tilde{F}_{\mu\nu}^a$ whose explicit color and Lorentz structure is given in Ref. [9]. For stability we must have $\lambda>0$. Evidently $\tilde{F}$ plays the role of a Higgs field and $W(\tilde{F})$ that of a Higgs potential. The minimum of W always occurs at a nonzero value $\tilde{F}_{0\mu\nu}$ of $\tilde{F}_{\mu\nu}$:

$$\frac{\delta W}{\delta\tilde{F}_{\mu\nu}} = 0 \quad \text{at } \tilde{F}_{\mu\nu}=\tilde{F}_{0\mu\nu} \ . \tag{2.15}$$

Let us digress briefly from our discussion of the potential between static quarks to elaborate a bit on the situation without quark sources; that is, on the properties of the dual QCD spontaneously broken vacuum. It is the fact that $\tilde{F}_0^2\neq 0$ in the vacuum which is responsible for spontaneous symmetry breakdown leading to dual superconductivity. (We take $\mu^2<0$ so that $-\tilde{F}_0^2>0$.) We can then choose $\bar{E}_0^2=0$ so that, from Eq. (2.14),

$$-\tilde{F}_0^2 = 2\mathbf{B}_0^2 \ . \tag{2.16}$$

Furthermore, we can set $\mathbf{E}^2=0$ in $\mathcal{L}(C)$ which amounts to making the replacement

$$\tilde{F}_{\mu\nu}\mathcal{D}^2\tilde{F}_{\mu\nu} \to -2\mathbf{B}\mathcal{D}^2\mathbf{B} \tag{2.17}$$

in Eq. (2.9). This eliminates terms in $\mathcal{L}$ which have the wrong sign of the kinetic energy and leads to a unitary theory. [The presence of an additional term in an earlier form of $\mathcal{L}(C)$ necessitated the introduction of the fields $\mathbf{E}$; we left them in Eq. (2.9) in order to make contact with this work.] In practice, we make the replacement (2.17) in (2.9), and replace $W(\tilde{F})$ by $W(\tilde{B})$. We shall retain the notation $-\tilde{F}_0^2$ for $2\mathbf{B}_0^2$.

In matrix notation, the explicit color structure of $\mathbf{B}_0$ is [9]

$$\mathbf{B}_0 = \left[\frac{-\tilde{F}_0^2}{N(N^2-1)}\right]^{1/2}(\hat{\mathbf{e}}_x J_1+\hat{\mathbf{e}}_y J_2+\hat{\mathbf{e}}_z J_3) \ , \tag{2.18}$$

where J_1, J_2, and J_3 are three SU(N) matrices having the form of matrices describing angular momentum j where $2j+1=N$. The matrices are normalized so that

$$2\,\mathrm{tr}\mathbf{B}_0^2 = \mathbf{B}_0^a\cdot\mathbf{B}_0^a \equiv B_0^2 \ . \tag{2.19}$$

Taking the trace of (2.18) then yields (2.16). For SU(3) we choose $J_1=\lambda_7$, $J_2=-\lambda_5$, $J_3=\lambda_2$. We also choose a representation in which J_3 is diagonal. Then, since the eigenvalues of J_3 are distinct, any matrix commuting with J_3 is diagonal. However, there are no diagonal matrices which commute with both of the angular momentum matrices J_1 and J_2. Therefore, there is no SU(N) matrix which commutes with all three vacuum fields B_{0x}, B_{0y}, and B_{0z}. Thus, all the (N^2-1) dual potentials C_μ^a obtain a mass

$$M^2 \sim g^2(-\tilde{F}_0^2) \ . \tag{2.20}$$

Of the $3(N^2-1)B^a$ fields, $2(N^2-1)$ become massive, while (N^2-1) remain massless and become the longitudinal components of the potentials C_μ^a. This is the dual of the mechanism whereby the photon obtains a mass in a superconductor. The mass M_B of the B field is of the order

$$M_B^2 \sim \lambda(-\tilde{F}_0^2) \ . \tag{2.21}$$

The fields B^a play the role of Higgs fields in the adjoint representation. The nonvanishing of $\mathbf{B}_0^2$ then gives rise to classical electric vortex solutions of the field equations derived from $\mathcal{L}$. Explicit solutions having one unit of quantized electric SU(3)-color flux are given in Ref. [9]. The energy per unit length, i.e., the string tension σ, has the form [9]

$$\sigma = (-\tilde{F}_0^2) f\left[\frac{\sqrt{\lambda}}{g}\right] , \tag{2.22}$$

where f is a dimensionless function of λ/g^2. λ/g^2 plays the same role in dual QCD that the Landau-Ginzburg parameter does in superconductivity. The square radius R^2 of the flux tube is of order

$$R^2 \sim -1/\lambda\tilde{F}_0^2 \ . \tag{2.23}$$

Fitting to experiment [9] yields the values

$$(-\tilde{F}_0^2) \sim (420\,\mathrm{MeV})^2, \quad \lambda \sim 1.6, \ g^2 \sim 8 \ . \tag{2.24}$$

To summarize, the classical approximation yields a flux tube containing one unit of SU(3)-color electric flux. This flux tube will confine a quark-antiquark pair attached to its ends, and thus dual QCD in the classical approximation explains quark confinement.

We next note that, for fixed $(-\tilde{F}_0^2)$, if

$$\lambda \to \infty$$

and

$$g^2 \to \infty \ , \tag{2.25}$$

with λ/g^2 finite, we obtain

$$M^2 \to \infty, \quad M_B^2 \to \infty, \quad \sigma \to \text{finite} \ . \tag{2.26}$$

Thus, in the strong-coupling limit, the only excitation in dual QCD is the flux tube. Furthermore, from Eq. (2.23) we see that, in this limit, the radius of the flux tube approaches zero, i.e., the flux tube becomes a string. (Perhaps this string theory could become a starting point for an approximation scheme for dual QCD.)

We now return to the problem of solving the equations of dual QCD in the presence of quark sources. At large distances the solution of these equations must be a gauge transformation of the vacuum configuration; $C_m = 0$, $\mathbf{B} = \mathbf{B}_0$: thus,

$$C_\mu \to \frac{i}{g}\Omega^{-1}\partial_\mu\Omega \ , \tag{2.27}$$

$$\mathbf{B} \to \Omega^{-1}\mathbf{B}_0\Omega \ , \tag{2.28}$$

where Ω is an SU(N) matrix, which we choose to be

$$\Omega = e^{-inY\varphi}, \quad n = 0, 1, \ldots, N-1 \ . \tag{2.29}$$

Here the SU(N) matrix Y satisfies

$$e^{-2\pi i n Y} = e^{-2\pi i n/N} \tag{2.30}$$

in order to guarantee that $\mathbf{B}$ is single valued. For SU(3),

$$Y = \frac{1}{\sqrt{3}}\lambda_8 \ . \tag{2.31}$$

From Eqs. (2.27) and (2.29) we obtain

$$\mathbf{C} \to -\frac{nY\hat{\mathbf{e}}_\phi}{g\rho} \quad \text{as } \rho \to \infty \ , \tag{2.32}$$

$$C_0 \to 0 \quad \text{as } \rho \to \infty \ . \tag{2.33}$$

The corrections to Eqs. (2.32) and (2.33) must vanish exponentially as $\rho \to \infty$.

In the absence of quark sources, the asymptotic behavior (2.32) corresponds to a vortex carrying n units of Z_N flux or, equivalently (with our choice of gauge), n units of flux of $\mathbf{D} = \nabla \times \mathbf{C}$. The vector potential $\mathbf{C}$ obtained in the $n = 1$ flux-tube solution of Ref. [9] gives

$$\oint \mathbf{C} \cdot d\mathbf{l} = \frac{2\pi}{g} Y = eY \ , \tag{2.34}$$

where the integral is around a large circle surrounding the flux tube.

In the case of interest, where sources are present, this unit of flux passes from the quark to the antiquark. However it is compensated by the contribution of the Dirac string in $\nabla \times \mathbf{C}$ because of our choice for $\mathbf{C}_D$ in which the string joins the charges. There is then no net flux of $\nabla \times \mathbf{C}$ crossing any plane perpendicular to the z axis. Equation (2.32) therefore gives $n = 0$, and from Eq. (2.29), $\Omega = 1$.

Aside from this difference, the color structure for $\mathbf{B}$ and $\mathbf{C}$ at all distances is the same as for the SU(3) $n = 1$ flux tubes. We have [9]

$$\mathbf{C} = C\hat{\mathbf{e}}_\phi Y \ , \tag{2.35}$$

$$\mathbf{B} = B(\hat{\mathbf{e}}_x J_x + \hat{\mathbf{e}}_y J_y) + B_e \hat{\mathbf{e}}_z J_z \ , \tag{2.36}$$

where C, B, and B_3 are functions of ρ and z. Comparing Eqs. (2.35) and (2.32) for $n = 0$ gives the long-distance boundary condition

$$C \to 0 \quad \text{faster than } 1/\rho \ , \tag{2.37}$$

as z or $\rho \to \infty$. Similarly, comparing Eqs. (2.18), (2.28), and (2.36) yields

$$B \to \left[\frac{-\tilde{F}_0^2}{N(N^2-1)}\right]^{1/2}, \qquad B_3 \to \left[\frac{-\tilde{F}_0^2}{N(N^2-1)}\right]^{1/2} , \tag{2.38}$$

as z or $\rho \to \infty$.

We now are in a position to write down the equations of motion for C, B, and B_3. It is convenient for this purpose to decompose C into the Dirac part and a leftover part c:

$$C = c + C_D \ , \tag{2.39}$$

then, as ρ or $z \to \infty$,

$$c \to -C_D \ . \tag{2.40}$$

In contrast, the amplitude C_{FT} of the vector potential for

the $n=1$ flux tube behaves asymptotically like [see Eq. (2.32)]

$$C_{\rm FT}\rightarrow -\frac{1}{\rho g} \text{ as } \rho\rightarrow\infty \ . \tag{2.41}$$

Furthermore, we will see that the equations for c can be obtained by making the replacement

$$\frac{1}{\rho g}\rightarrow C_D \tag{2.42}$$

in the equations for $C_{\rm FT}$ given in Ref. [9].

We note that

$$\nabla\times(\nabla\times\mathbf{C}_D+\mathbf{D}_S)=0 \ , \tag{2.43}$$

since $\nabla\times\mathbf{C}_D+\mathbf{D}_S$ is nothing but the field due to a point charge [see Eq. (2.5)]. Hence,

$$\nabla\times(\nabla\times\mathbf{C}+\mathbf{D}_S)=\nabla\times(\nabla\times\mathbf{c}) \ . \tag{2.44}$$

Next, in writing down the field equations, as well as in carrying out the numerical solutions of them, it will be convenient to scale certain factors out of the fields, as was done in Ref. [9]. We define

$$\rho'=(-\lambda\tilde{F}_0^2)^{1/2}\rho \ , \tag{2.45a}$$

$$C'=(-\tilde{F}_0^2)^{-1/2}C \ , \tag{2.45b}$$

$$B'=(-\tilde{F}_0^2)^{-1/2}\left[\frac{N(N^2-1)}{6}\right]^{1/2}B \ , \tag{2.45c}$$

$$B'_3=(-\tilde{F}_0^2)^{-1/2}\left[\frac{N(N^2-1)}{6}\right]^{1/2}B_3 \ , \tag{2.45d}$$

where, of course, $N=3$ for SU(3) of color. We also define

$$g'=g/\sqrt{\lambda} \ . \tag{2.46}$$

Finally, after all of these remarks, the Lagrangian is

$$\mathcal{L}=\lambda(\tilde{F}_0^2)^2[\tfrac{2}{3}c'\tilde{\nabla}'^2c'+B'\nabla'^2B'+\tfrac{1}{2}B'_3\nabla'^2B'_3 -g'^2B'^2(c'+C'_D)^2-W'] \tag{2.47}$$

and the resulting field equations are

$$\tfrac{4}{3}\tilde{\nabla}'^2c'-2g'^2B'^2(c'+C'_D)=0 \ , \tag{2.48a}$$

$$\nabla'^2B'-g'^2(c'+C'_D)^2B'=\frac{1}{2}\frac{\partial W'}{\partial B'} \ , \tag{2.48b}$$

$$\nabla'^2B'_3=\frac{\partial W'}{\partial B'_3} \ . \tag{2.48c}$$

Here

$$\nabla^2=\frac{1}{\rho}\frac{\partial}{\partial\rho}\rho\frac{\partial}{\partial\rho}+\frac{\partial^2}{\partial z^2} \tag{2.49}$$

and

$$\tilde{\nabla}^2=\nabla^2-\frac{1}{\rho^2} \ . \tag{2.50}$$

The boundary conditions are that, at infinity, $c'\rightarrow -C'_D$, and both B' and $B'_3\rightarrow\sqrt{1/6}$ [this because of the choice of normalization (2.17)]. These are simply the result of requiring that B and B_3 approach the physical vacuum in the dual superconductor and that C vanish at a large distance from the quark-antiquark pair. The remaining boundary conditions are that c vanishes on the z axis, while the behavior of B is determined by the behavior of C_D as $\rho\rightarrow 0$. For $|z|<R/2$, between the quark-antiquark pair, $C_D\sim 1/\rho$ as $\rho\rightarrow 0$ forcing B to vanish on the z axis; however, outside of this interval C_D vanishes as $\rho\rightarrow 0$ and the radial derivative of B must therefore vanish on this portion of the axis. Finally, B_3 approaches a constant along the entire z axis.

Once these field equations are solved numerically, it is a simple matter to extract the total energy of the system; that is, the static potential between quarks.

Recalling Eq. (2.8), and using Eq. (2.22b) of Ref. [9], we find (dropping self-energies) that

$$V=\int d^3\mathbf{x}\,\mathcal{H}=\frac{4}{3}\left[-\frac{e^2}{4\pi R}\right]+\lambda(\tilde{F}_0^2)^2\int d^3\mathbf{x}'\left[W'-\frac{1}{2}B'\frac{\partial W'}{\partial B'}-\frac{1}{2}B'_3\frac{\partial W'}{\partial B'_3}-g'^2B'^2c'(c'+C'_D)+\frac{1}{9}\right] , \tag{2.51}$$

where

$$\int d^3\mathbf{x}'=2\pi\int_0^\infty\rho'\,d\rho'\int_{-\infty}^{\infty}dz' \ . \tag{2.52}$$

It is gratifying that the factor $\frac{4}{3}$, characteristic of classical static sources in SU(3) [7], appears automatically in front of the Coulomb energy. This results from $\frac{4}{3}$ in Eq. (2.19a), which, in turn, follows from the fact that $\mathbf{C}$, and hence also $\mathbf{C}_D$, have been assumed to be in the λ_8 direction in color. This, we recall, was required because, in the sourceless flux tube, $\mathbf{C}$ proportional to λ_8 is necessary in order to have a tube carrying a single unit of quantized electric flux.

III. NUMERICAL SOLUTION OF THE FIELD EQUATIONS

The evident symmetry under the transformation $z\rightarrow -z$ means that the complete solution can be obtained by considering only the half space $z>0$ with appropriate

boundary conditions. c, B, and B_3 are all even in z; as a result, at $z=0$,

$$\frac{\partial c}{\partial z}=\frac{\partial B}{\partial z}=\frac{\partial B_3}{\partial z}=0 \ . \tag{3.1}$$

The two-dimensional area $0<\rho<\rho_{\max}$ and $0<z<z_{\max}$ is discretized on a rectangular $n\times m$ mesh. Using the standard central difference approximations for the derivatives, the field equations become difference equations on this lattice. The fact that the dynamical fields fall with a known exponential behavior at large z and ρ allows one to estimate the values of $\rho_{\max}$ and $z_{\max}$ necessary to produce a sufficiently accurate solution. In practice, we varied these quantities to show that the quantities of physical interest, such as the string tension, were, in fact, independent of the cutoff values.

The numerical solution of the difference equations was obtained by using the Gauss-Seidel method with the successive overrelaxation (SOR) technique following the general procedures recommended by Adler and Piran [10]. The procedure was as follows. One began with a small lattice, typically 8×8, with a guess for the first trial solution which was iterated until convergence was obtained. These solutions were then interpolated to provide a trial solution on a 16×16 lattice. Once the solution on this lattice had been obtained, it, in turn, was used to provide a trial solution on a larger lattice. Because the trial functions on the large lattices were close to the actual solutions, the convergence was generally quite rapid. In most cases a rectangular rather than a square lattice was used because, as the quark-antiquark separation was increased, it was necessary to increase $z_{\max}$, requiring the use of more mesh points in the z than in the ρ direction to maintain a similar resolution in each variable. The maximum change of the fields during a single Gauss-Seidel iteration was used as the criterion for convergence. For small lattices, the order of 50 iterations was required to obtain solutions of sufficient accuracy for interpolation to the next larger lattice. For the largest lattice, it was possible to iterate until the solution was stable to machine accuracy (double precision on an IBM RS6000). In most cases, the iteration was stopped after the fields stabilized to six significant figures. For lattices with less than 10 000 lattice points, 200–400 iterations were used.

At each change of lattice, the number of points was increased by a factor of 4. This procedure not only proved to be an efficient method of obtaining the solution for a large lattice but also gave information on the lattice-

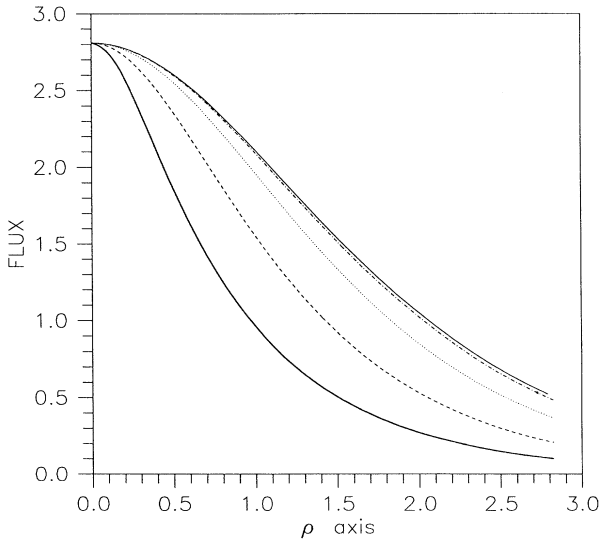

FIG. 1. Flux through circles in the median plane as a function of radius for various quark-antiquark separations. Note that the value at zero radius, which is the flux carried by the string, is $2\pi/g'$ with $g'=\sqrt{5}$ (see Ref. [9]). The heavy solid line is for sources at ± 0.5, the dashed line ± 1.0, the dotted line ± 2.0, and the dot-dashed line ± 4.0. The thin solid line is for sources at infinity.

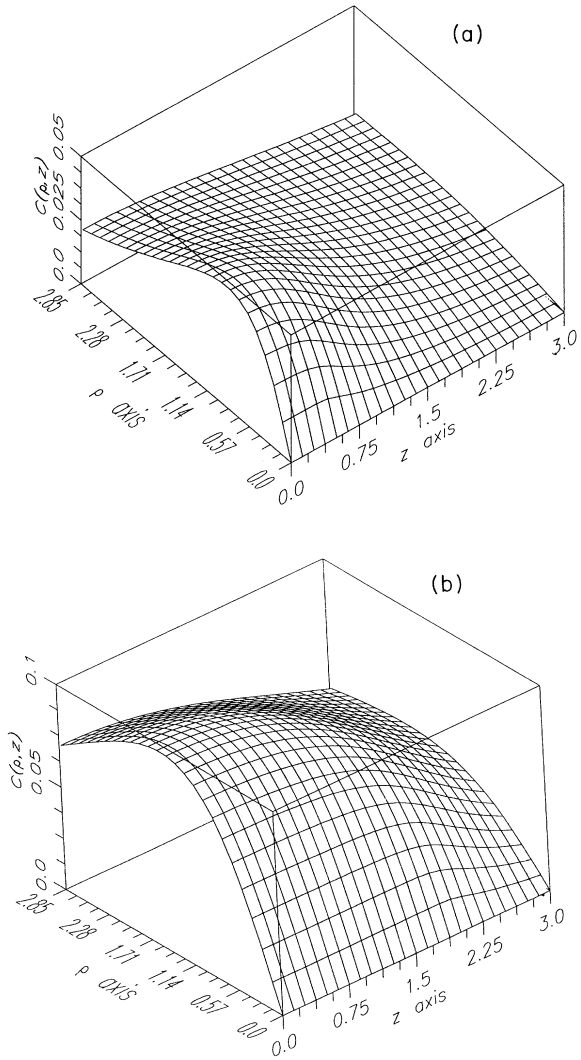

FIG. 2. The dual potential C as a function of ρ and z for separations of (a) 1 unit and (b) 4 units. Note that the C-axis scales in (a) and (b) are different.

spacing dependence of the relevant physical quantities such as the quark-antiquark interaction energy. This information allowed us to estimate how large a lattice was necessary to provide a stable result and, in fact, could be used in a Richardson-type [11] extrapolation to zero-lattice spacing to obtain the continuum values for the quantities of interest.

The final step in this procedure was to vary $z_{\max}$ and $\rho_{\max}$ to verify that these parameters were large enough so that the interaction energy was independent of these cutoffs.

The potential calculated in this way blends smoothly into the flux-tube solution (though, of course, for the flux-tube solution we must insert an axial string so that it carries a net zero single unit of quantized flux at infinity), obtained previously [9]. This provides a check on the validity of the numerical procedures used here. Figure 1 shows the flux through a circle in the median plane (including the string contribution) as a function of circle radius for various quark-antiquark separations. The separation $=\infty$ curve is the result of the flux-tube calculation of Ref. [9]. As one can see from the figure, the asymptotic value is not reached until the quark and antiquark are separated by about 8 (in our dimensionless units). (The string carries one unit e of quantized flux. Since $e=2\pi/g$, the value appearing at the origin in Fig. 1 is $2\pi/g'$ and corresponds to the choice $g'=\sqrt{5}$ which we found in Ref. [9].)

IV. RESULTS

Figures 2–4 show the fields C, B, and B_3, respectively, for separations 1 and 4 between the sources, as functions of the cylindrical coordinates ρ and z. Note that B_3 is essentially independent of everything—both coordinates and source separation. It can obviously be taken to be a constant to a high degree of accuracy.

The other two fields vary considerably in space. The variation is quite smooth, for both separations, suggesting that bag models of the quark-antiquark potential may

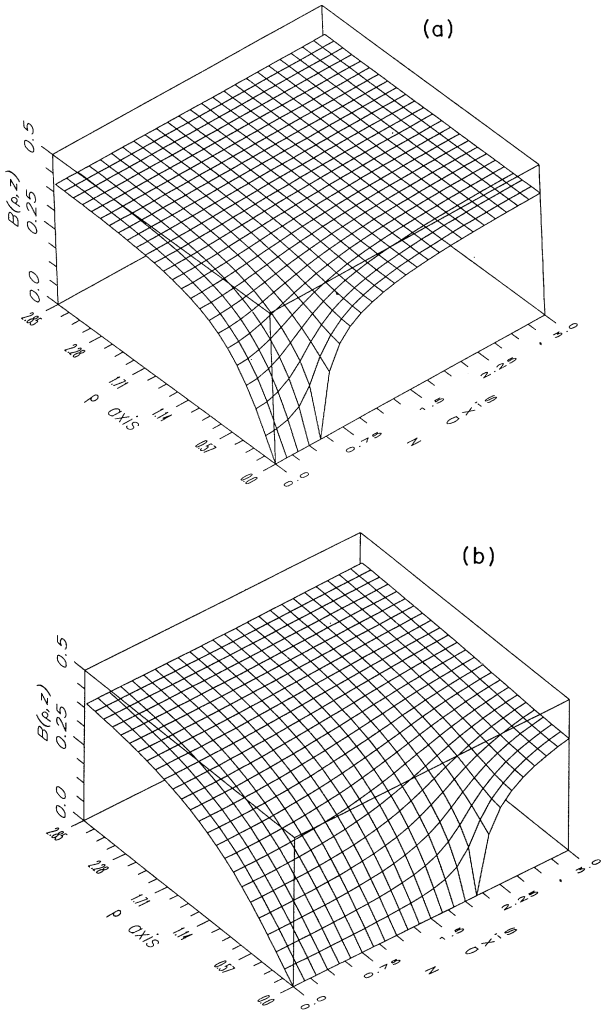

FIG. 3. The field B as a function of ρ and z for separations of (a) 1 unit and (b) 4 units.

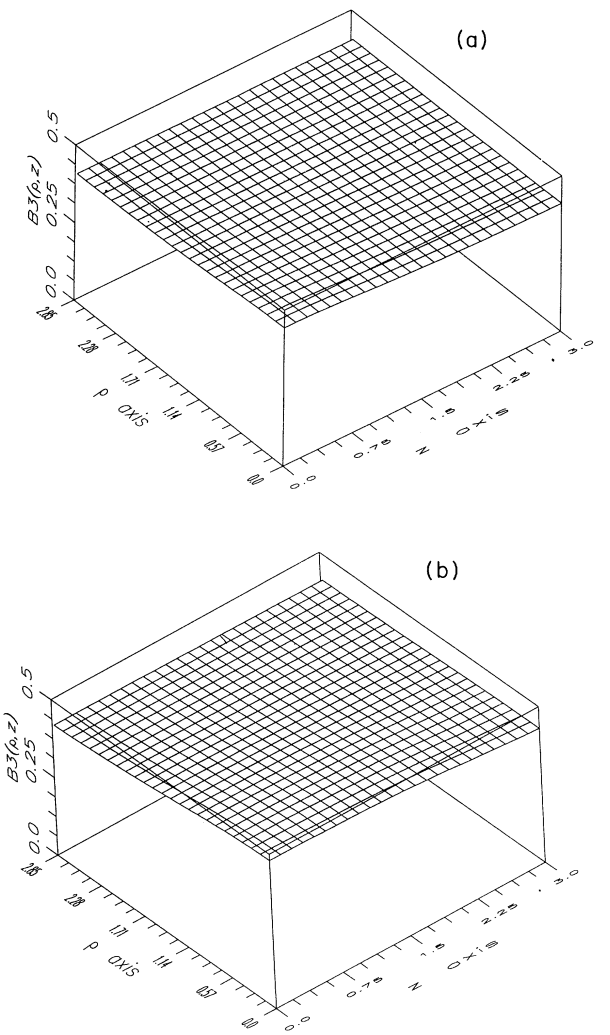

FIG. 4. Again, the same plot, now for B_3.

not be very accurate. The boundaries of the regions where the fields differ from their asymptotic values (recall that $B \to b$ as ρ and/or $z \to \infty$) are by no means sharp, but cover a distance of the same order as the entire region containing flux itself. Figure 3 shows that, as required, the transverse magnetic field B vanishes on the z axis between the two charges, and then rises quite rapidly to its nonzero asymptotic value as either ρ or z is increased. It should be noted that the plots of both B and B_3 are of gauge-invariant quantities. The gauge-invariant axial magnetic field is $\sqrt{B_3^a B_3^a} = B_3$.

Figure 5 shows the lines of electric displacement, **D**, for separations of 1, 2, 4, and 8 units between the quark and antiquark. The lines form boundaries of regions of equal flux. One can clearly follow the smooth evolution of the field configuration from what almost looks like a squashed dipole for sources at $\pm\frac{1}{2}$ to what has become a long sausage, and will eventually become an infinite flux tube, when the sources are at $=4$. Again it is worth emphasizing the smooth variation of the **D** field from the region where flux exists to where it does not.

The static potential obtained from these solutions, using Eq. (2.22), is shown in Fig. 6, as is the phenomenological $q\bar{q}$ potential of Ref. [7]. The parameter used in the calculation is $g' = \sqrt{5}$ (the value used in Ref. [9]), but the potential and the distance scale have been restored to conventional units using Eq. (2.17) with $\lambda = 1.61$, $(-\tilde{F}_0^2)^{1/2} = 420$ MeV, and, of course, $N = 3$ as is appropriate to SU(3). The agreement is, evidently, excellent. There seems to be a very slight deviation in the asymptotic slope (i.e., the string tension). This results from our use of the string tension from Ref. [9], and the

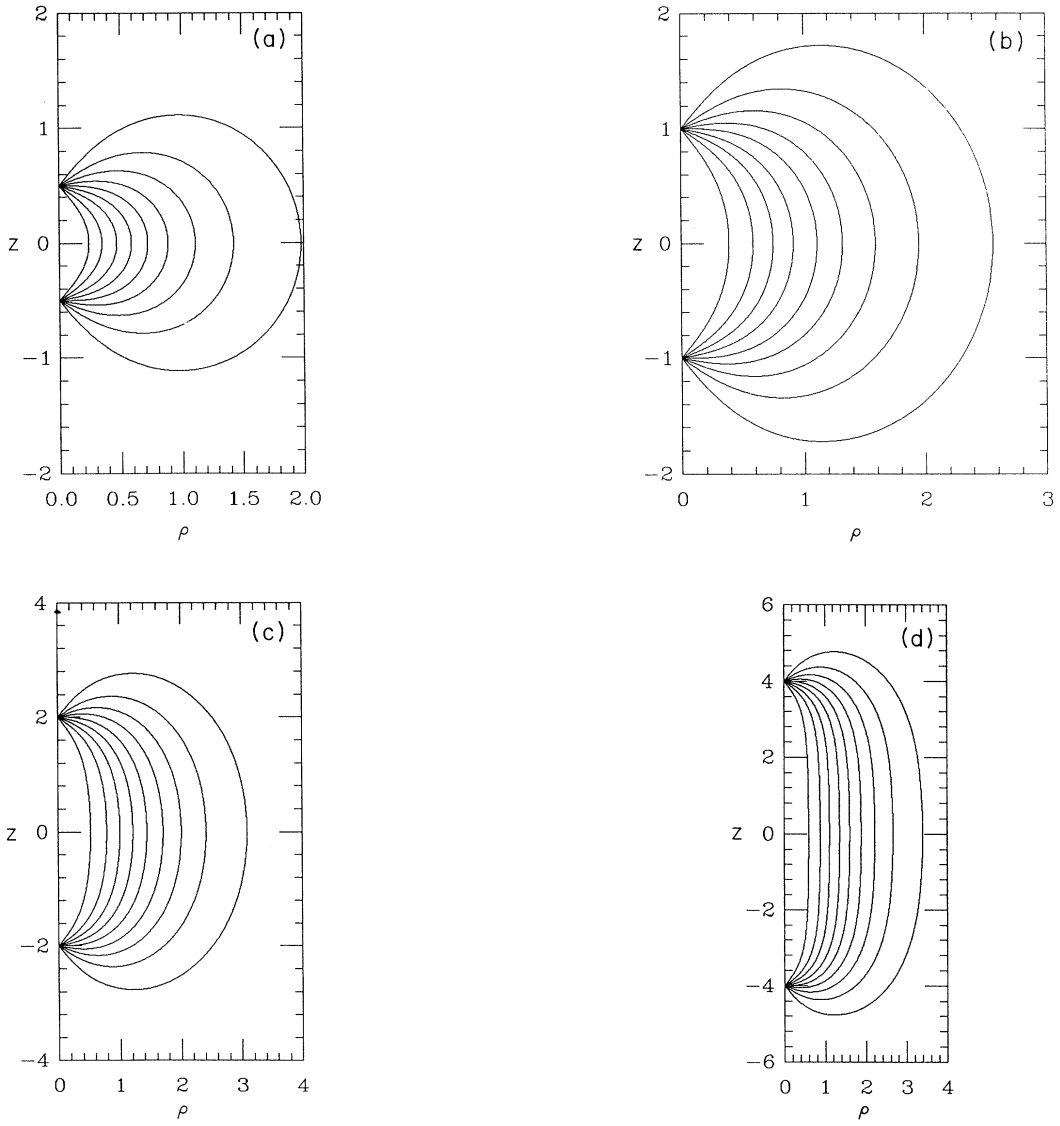

FIG. 5. (a) The lines of **D** for quark and antiquark sources at $\pm\frac{1}{2}$. (b), (c), and (d) show the same thing when the sources are located at ± 1, ± 2, and ± 4, respectively.

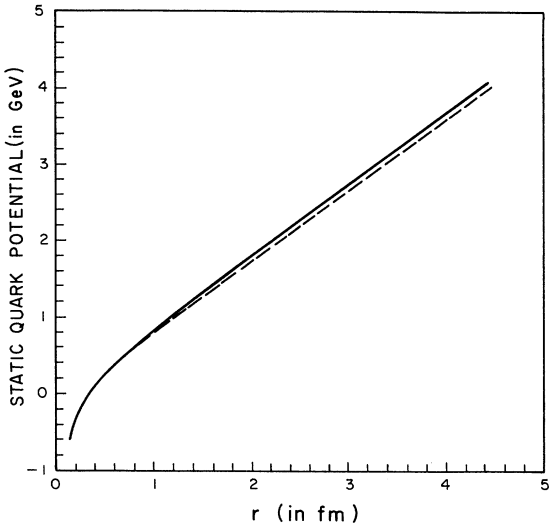

FIG. 6. Static quark-antiquark potential as a function of source separation. The dotted line is the phenomenological potential of Ref. [7].

value $g'=\sqrt{5}$, and could, if we so desired, probably be fine-tuned a bit. It is interesting to note that our potential is well approximated by the sum of the linear string tension term, an exponential factor times the Coulomb term and a constant. This form undergoes a rather rapid transition from a region in which it behaves like $1/R$ to one in which it behaves like R.

V. CONCLUSION

We have calculated using dual QCD in the classical approximation the distribution of color fields around a static quark-antiquark pair and have shown how a flux tube evolves as their separation increases. For separations (in units of the flux-tube radius) much smaller than one, the field lines have the appearance of a squashed dipole distribution. For larger separations the field lines continue to flatten but, even at a separation of 4 units, the field lines have curvature at the median plane. At separations of about 8 units a central region having field lines parallel to the z axis finally develops in the region between $z=-2$ and $+2$. The fields in this region are those of a flux tube. However, the potential between the quark-antiquark pair already becomes linear when the separation between the quark-antiquark pair is only 2 units, well before the appearance of a fully developed flux tube. This rapid transition to a linear potential also occurs in the bag model. However, no evidence of anything approximating a sharp boundary, such as the bag model assumes, is visible.

Haymaker and Wosiek [12] have calculated the distribution of color fields around static quarks in SU(2) and found the resulting potential in lattice QCD. Their results give a similar picture to those obtained in this paper. More precise lattice calculations of SU(3)-color field distributions would make possible a more quantitative comparison with our results and could test quantitatively whether dual superconductivity is the physical mechanism for confinement in QCD.

The numerical calculations carried out in this paper are not difficult and display no unwanted singularities or other phenomena. This suggests that methods analogous to those described here can also be used to calculate static spin dependent potentials between heavy quarks and antiquarks and, in fact, such works are in progress.

ACKNOWLEDGMENTS

The work of M.B. was supported in part by the U.S. Dept. of Energy under Contract No. DOE/ER/40614. The work of J.S.B. was supported in part by the U.S. National Science Foundation Grant No. PHY 9008482. The work of F.Z. was supported in part by the U.S. Dept. of Energy under Contract No. DEAC-03-81ER40050.

[1] M. Baker, James S. Ball, and F. Zachariasen, Phys. Rev. D **37**, 1036 (1988).
[2] M. Baker, James S. Ball, and F. Zachariasen, Phys. Rev. D **44**, 2578 (1991).
[3] James S. Ball and Ariel Caticha, Phys. Rev. D **37**, 524 (1988).
[4] See, for example, C. DeTar and J. Donoghue, Annu. Rev. Nucl. Sci. **33**, 235 (1983); P. Hasenfratz and J. Kuti, Phys. Rep. **40C**, 75 (1978).
[5] M. Baker, James S. Ball, and F. Zachariasen, Phys. Rev. D **34**, 3894 (1986).
[6] H.-Q. Ding, C. F. Baillie, and G. C. Fox, Phys. Rev. D **41**, 2912 (1990); M. Caselle, R. Fiore, and F. Gliozzi, Phys. Lett. B **224**, 153 (1989).
[7] E. Eichten *et al.*, Phys. Rev. D **21**, 203 (1980).
[8] M. Baker, James S. Ball, and F. Zachariasen, Phys. Rev. D **38**, 1926 (1988).
[9] M. Baker, James S. Ball, and F. Zachariasen, Phys. Rev. D **41**, 2612 (1990).
[10] S. Adler and T. Piran, Rev. Mod. Phys. **56**, 1 (1984).
[11] See, for example, E. L. Burden and J. D. Faires, *Numerical Analysis*, 3rd ed. (PWS, Boston, 1985).
[12] R. W. Haymaker and J. Wosiek, Phys. Rev. D **43**, 2676 (1991).